Differential Scanning Calorimetric Examination of Melamine–Formaldehyde Microcapsules Containing Decane

Branko Alič, Urška Šebenik, Matjaž Krajnc

Faculty of Chemistry and Chemical Technology, University of Ljubljana, Aškerčeva Cesta 5, SI-1001 Ljubljana, Slovenia

Received 13 May 2010; accepted 19 July 2010
DOI 10.1002/app.33077
Published online 30 September 2010 in Wiley Online Library (wileyonlinelibrary.com).

ABSTRACT: The main objective of this study was to investigate the composition of microcapsules and the degree of curing of melamine–formaldehyde (MF) resin, which formed a shell of microcapsules, by the use of differential dynamic calorimetry (DSC). For this purpose, decane was chosen as core material. The microencapsulation of decane with MF resin was carried out at different temperatures and pH values. The temperature and pH value were kept constant during the process. The composition of the microcapsules and the degree of curing of the shell material were studied during and after the microencapsulation process. DSC analysis, in combination with scanning electron microscopy analysis, was revealed as an effective tool for the investigation of the microencapsulation process with MF resin. © 2010 Wiley Periodicals, Inc. J Appl Polym Sci 119: 3687–3695, 2011

Key words: crosslinking; differential scanning calorimetry (DSC); electron microscopy; microencapsulation; polycondensation

INTRODUCTION

Microcapsules are tiny particles with diameters in the range between 1 and 1000 μm that consist of a core material and a covering shell. The core material can be solid, liquid, or gas. The shell material is usually a synthetic or natural polymer. Through the selection of the core and shell material, it is possible to obtain microcapsules with a variety of functions. This is why they can be defined as containers that can release, protect, and/or mask various kinds of active core materials.[1]

Microencapsulation processes can be largely divided into chemical processes, physicochemical processes, and mechanical processes. *In situ* processes, such as suspension, emulsion, precipitation, or dispersion polymerization, and interfacial polycondensation are the most important chemical techniques used for microencapsulation. Polycondensation processes, which may be either normal dispersion polycondensations or interfacial polycondensations, are especially attractive for liquid core materials (active agents). In dispersion polycondensation, the monomers are initially soluble in the polymerization medium, whereas the active agent is in the emulsion form. As the polymerization reaction begins in a homogeneous solution, oligomers collapse on the surface of the active agent droplets and grow into a polymer that encloses the active agent.[1–3]

Melamine–formaldehyde (MF) microcapsules can be prepared by the *in situ* polymerization process by polycondensation, which allows the formation of microcapsules containing water-immiscible core materials, such as fragrant oils,[4–7] flavors,[8] self-healing agents,[9–12] fire retardants,[13–15] and phase-change materials.[16–22] The properties of the MF shell depend not only on the MF resin chemical structure, such as the melamine-to-formaldehyde molar ratio,[4,23] or MF resin chemical modification or functionalization but also on the core-to-shell mass ratio[20] and on the microencapsulation process parameters, such as stirring conditions,[3,7,9,24–27] pH value,[4,14,23] and temperature.[4,14,25,28] The polymerization of MF resin occurs exclusively in the continuous water phase and on the continuous phase side of the interface formed by the dispersed core material and continuous phase. The polymerization of MF resin produces prepolymer of relatively low molecular weight in the continuous phase. As the prepolymer molecular weight increases, it deposits on the surface of the dispersed phase being encapsulated. On the surface, the polymerization continues, and crosslinking occurs. With crosslinking, a solid MF shell is formed.[2,4,29,30] The separation by which the microcapsule shell is

Correspondence to: M. Krajnc (matjaz.krajnc@fkkt.uni-lj.si).

Contract grant sponsor: Slovenian Ministry of Higher Education, Science and Technology; contract grant number: P2-0191.

formed is particularly linked to the pH value,[4,14,23] temperature,[10] type, and amount of emulsifier used[9,10,25–27,31–34] and to the melamine-to-formaldehyde molar ratio. It significantly determines the encapsulation efficiency and shell morphology.[4,18,30,31,35–37] The addition of a shell material to a water dispersion of core material in one step is the most used method, although it has been observed[18,21,22] that microcapsules prepared by the addition of a shell material in two steps were mechanically and thermally more stable. Despite the fact that microencapsulation process parameters have a significant effect on the encapsulation efficiency and shell morphology,[9,26,35] published research works dealing with this problem are rare. Even fewer research groups have investigated the composition of microcapsules and the degree of curing of shell material during the microencapsulation process. Most of the articles are focused on the preparation of different microcapsules at constant process parameters and on end-product characterization by the use of different instrumental techniques, such as differential scanning calorimetry (DSC),[38] thermogravimetric analysis,[38] Fourier transform infrared spectroscopy, transmission electron microscopy, scanning electron microscopy (SEM), and laser diffraction. Dubernet[38] described different cases in which the use of DSC allows researchers to obtain more information about the internal structure of microcapsules, especially with regard to the nature of the interaction between the polymer matrix and the encapsulated drug. In this study, the microencapsulation of decane with MF resin was carried out at different temperatures and pH values, which were kept constant during the process. The main objective of this study was to investigate the composition of the microcapsules, that is, their shell-to-core weight ratio and the degree of curing of MF resin, which formed the shell of the microcapsules, by DSC. For this purpose, decane was chosen as core material. The composition of microcapsules and the degree of curing of the shell material were studied not only after the microencapsulation process but also during the process.

EXPERIMENTAL

Materials

Etherified MF resin (70 wt %, Melapret NF70/M, Melamin, Kočevje, Slovenia), decane (decane fraction, purum, Fluka, Chemika, Buchs, Switzerland), sodium dodecyl sulfate (≥96%, purum, Fluka), 5 wt % sodium hydroxide solution (99%, Merck, Darmstadt, Germany), 5 wt % acetic acid solution (99.8%, Merck), and deionized water were used.

Preparation of the microcapsules

Emulsion preparation

We mixed 20 g of decane, 10 g of sodium dodecyl sulfate (the emulsifier), and 370 g of deionized water using an Ultraturax Dispermat (VMA-Getzman, Reichshof, Germany) at a rate of 1000 rpm for 30 min at room temperature. Then, 100 g of a 14 wt % MF resin aqueous solution was added to the emulsified decane, and the mixture was mixed for additional 30 min. The emulsion pH value was adjusted to the desired value (5.0, 5.5, or 6.0) with a 5 wt % acetic acid solution.

Microencapsulation

The emulsion was poured into a glass reactor with four necks, equipped with a reflux condenser, mechanical stirrer, digital thermometer, and glass electrode for pH measurements. The reactor content was stirred at a rate of 500 rpm and heated to the desired temperature (40 or 50°C). The temperature and pH value of the reaction mixture were kept constant during the microencapsulation process. The pH value was adjusted to the desired value every 15 min with a 5 wt % sodium hydroxide solution and a 5 wt % acetic acid solution. During the microencapsulation process, several samples were taken from the reactor to investigate their composition and degree of MF resin curing. After 4 h, the reaction mixture was cooled to 25°C and the pH value was raised to 8.0 to terminate the reaction. The microencapsulation product was filtered through filter paper discs (Sartorius 388, Sartorius AG, Goettingen, Germany) and washed with deionized water. The wet cake-containing microcapsules were dried at room temperature to a constant weight, and dry powders of microcapsules were used for the characterization. In the text, the samples are labeled as MC/x/y, where MC stands for the microcapsules, x represents the temperature, and y represents the pH value during the microencapsulation process.

Characterization of the microcapsules

The morphology of the microcapsules was observed by SEM with a field emission scanning electron microscope (SUPRA 35VP, Carl Zeiss, Oberkochen, Germany). The sample was imaged with a 1-kV accelerating voltage. Before SEM analysis, volatile decane had to be removed from the samples. For this purpose, samples were dried *in vacuo* at room temperature; this also caused shell rupture and enabled shell thickness determination.

DSC was performed to characterize the thermal response properties of decane and MF resin in microcapsules prepared with different process parameters. The measurements were performed on a Mettler

Toledo DSC821e (Mettler Toledo, Zurich, Switzerland) instrument with an intracooler and using STAR software. In and Zn standards were used for the temperature calibration and for the determination of the instrument time constant. A nitrogen atmosphere and standard alumina pans were used. Methods of different temperature programs for different purposes were applied. To define the mass percentage of shell material in the microcapsules, standard 40-μL alumina pans were used, and the following DSC method was applied: cooling from 25 to −100°C at a cooling rate of −5°C/min and subsequent heating from −100 to 25°C at a heating rate of 5°C/min. The sample mass was about 10 mg. When the degree of curing of the MF resin, which formed a shell of microcapsules, was investigated, standard 160-μL alumina pans were used, and the following DSC method was applied: heating from 100 to 300°C at a heating rate of 2.5°C/min. The sample mass was about 10 mg.

To confirm the core-to-shell weight ratio obtained by DSC analysis, gravimetric analysis was also performed. About 1 g of a sample of microcapsules was weighed, and 45 mL of acetone was added. The samples were put in ultrasound bath at 50°C for 3.5 h; this enabled the rupture of the microcapsules. Then, the samples were dried at room temperature for 12 h and then for an additional 15 h *in vacuo* at 50°C to remove all of the solvent and decane. The dried samples were weighed, and the mass percentage of the shell material in the microcapsules was calculated.

RESULTS AND DISCUSSION

Microcapsule morphology and composition

From SEM images, the microcapsule diameter, shell thickness, and morphology were evaluated. Selected images of the microcapsules prepared at different process parameters are shown in Figure 1. The estimated diameter of the microcapsules was between 35 and 55 μm for all of the samples. However, the shell thickness varied considerably with pH value. It was observed, that with increasing pH value, the shell thickness decreased (Table I) and the microcapsules with the thinnest shell were also the most damaged after their exposure to a vacuum. This is why no intact microcapsules and only damaged microcapsules shells were observed in the image of sample MC/40/6.0 [Fig. 1(f)]. For example, sample MC/50/5.5 contained less damaged microcapsules after its exposure to a vacuum [Fig. 2(a)]. An example of shell thickness determination for sample MC/40/5.0 is given in Figure 2(b). Small particles of different sizes attached to the shell surface, which are also shown in Figure 1, were assumed to be MF particles with only a small core or without a decane core because these particles were not damaged after exposure to a vacuum. We observed that the amount and size of small MF particles on the shell surfaces increased with decreasing pH value. Particularly, sample MC/40/5.0 [Fig. 1(b)] contained microcapsules with many small particles with diameters of around 1.3 μm on their surface. On the other hand, no small particles were observed in images of the sample prepared at the highest pH value and the lowest temperature [MC/40/6.0, Fig. 1(f)]. However, the surface of the microcapsules of sample MC/50/6.0 [Fig. 1(e)] was covered with some MF particles with a diameter of about 200 nm and many smaller particles that were not spherical in shape.

The 10°C difference in the reaction temperature did not significantly affect the particle morphology or shell thickness of the microcapsules prepared at pH values of 5.0 and 5.5. A significant difference in the shell thickness was observed only between samples MC/50/6.0 and MC/40/6.0, where the thinnest shells in the latter were observed (Table I).

To conclude, we observed small MF particles attached to the shell surface, but we did not observe the so-called polynuclear or raspberry-like surface morphology mentioned elsewhere,[4,14,30] even when the samples were prepared at a pH value of 5.0. We assumed that the raspberry-like surface morphology was prevented by the high emulsifier concentration and by the constant pH value of the continuous medium, which tended to decrease during the microencapsulation process.

By the use of DSC analysis, the mass percentage of the shell material in the microcapsules was determined. In addition to the end microcapsule composition, we followed the composition during the microencapsulation processes by sampling the reactor content at 30-min intervals and filtrating and drying it. The samples were analyzed in the temperature range where decane showed crystallization and melting peaks.

In Figure 3(a,b), thermograms for decane and the microcapsules obtained at the end of microencapsulation processes at 40 and 50°C and pH values of 5.0, 5.5, and 6.0 are shown. Decane enclosed in microcapsules crystallized at lower DSC cell temperatures and melted at higher DSC cell temperatures than pure decane. For both cases, crystallization and melting, sharper peaks for samples of pure decane were observed. The differences in the peak shape and width [Fig. 3(a,b)] were ascribed to different conditions for heat transport in the samples and to intermolecular interactions between decane and MF resin at the core–shell interfacial area. When decane was enclosed in MF shells, the delay observed for crystallization and melting was a consequence of heat transport through microcapsules shells. In other words, in the case when the pure decane sample was analyzed, the contact between decane and the DSC pan was much better. On the other hand, with increasing MF resin crosslinking degree, the ability

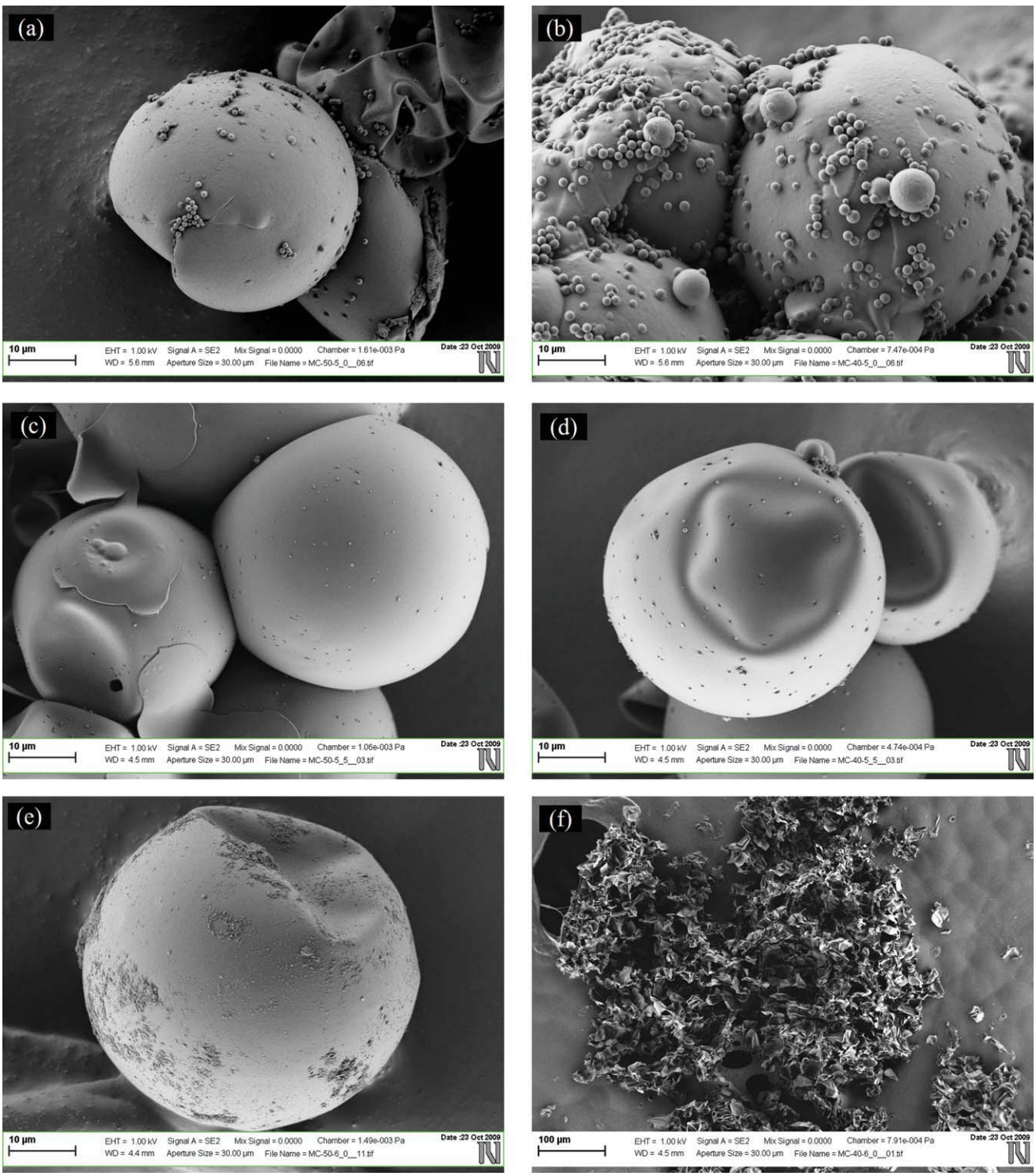

Figure 1 SEM images of microcapsules prepared with different process parameters: (a) MC/50/5.0, (b) MC/40/5.0, (c) MC/50/5.5, (d) MC/40/5.5, (e) MC/50/6.0, and (f) MC/40/6.0. [Color figure can be viewed in the online issue, which is available at wileyonlinelibrary.com.]

of MF resin to swell in decane decreased, and therefore, decane crystallization and melting were influenced to a lesser extent. This was observed in the shapes of the crystallization and melting peaks, shown in Figure 3(a,b). The lower the pH value was, the higher the MF resin crosslinking degree was and the closer the peaks of encapsulated decane to the peak of pure decane were. The shapes of the crystallization peaks for samples of microcapsules prepared at 40°C, which showed a small peak at higher temperature [Fig. 3(a)], were ascribed to decane, which was not enclosed in microcapsules. Because

TABLE I
Properties of Microcapsules Prepared with Different Process Parameters

	Decane	MC/40/6.0	MC/40/5.5	MC/40/5.0	MC/50/6.0	MC/50/5.5	MC/50/5.0
Shell thickness (nm)	—	~ 70	~ 200	~ 420	~ 130	~ 210	~ 440
Melting enthalpy (J/g)	−156.4	−146.7	−144.6	−125.8	−146.5	−146.4	−132.8
Mass percentage of the shell material	0	6.2	7.5	19.6	6.3	6.4	15.1
Curing enthalpy (J/g)	—	—	—	—	274	196	104

the samples were filtered, washed, and dried before the analysis, we believe that some capsules were damaged during sample handling for DSC analysis purposes. In these cases, not all of the decane was inside the microcapsules, and this resulted in the small peaks at higher temperatures.

To determine the accuracy and reproducibility of the DSC results, gravimetric analysis and five replicates of the DSC measurements were performed, respectively. The DSC and gravimetric measurements results for five replicates of sample MC/50/5.5, together with their average value and relative standard deviation, are shown in Table II. The DSC results agreed satisfactorily with the gravimetric results.

Variations in the mass percentage of the shell material in microcapsules during microencapsulations carried out with different process parameters are depicted in Figure 4. Here, for most cases, the results for times of 1.5 h and above are given because, before 1.5 h, the microcapsules were very fragile, and it was practically impossible to handle the samples without damaging them previous to

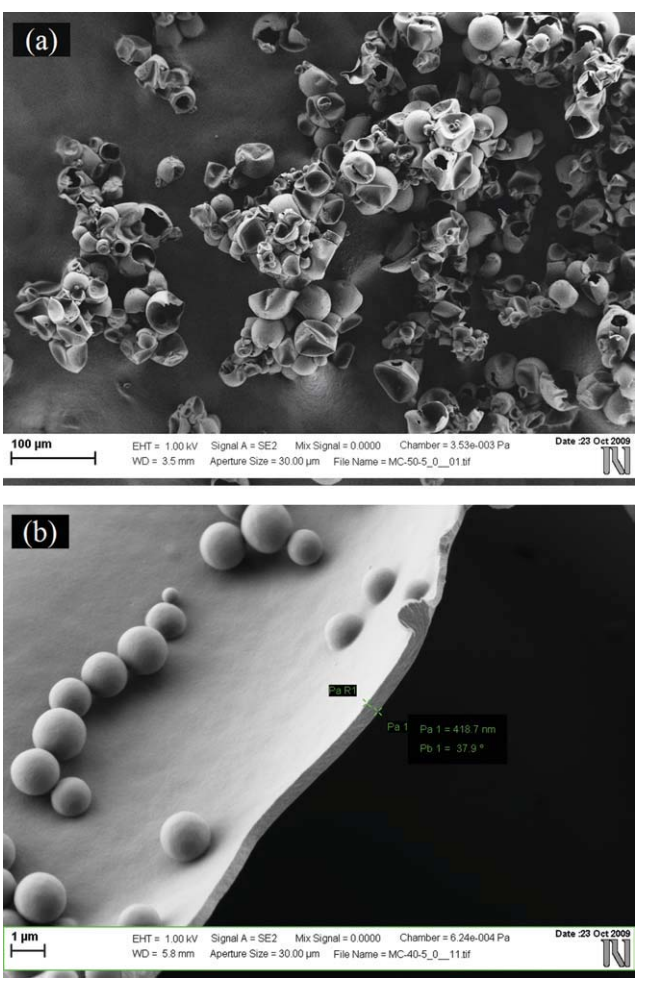

Figure 2 (a) SEM images of the damaged microcapsules after vacuum exposure for sample MC/50/5.0. (b) Shell thickness determination for sample MC/40/5.0. [Color figure can be viewed in the online issue, which is available at wileyonlinelibrary.com.]

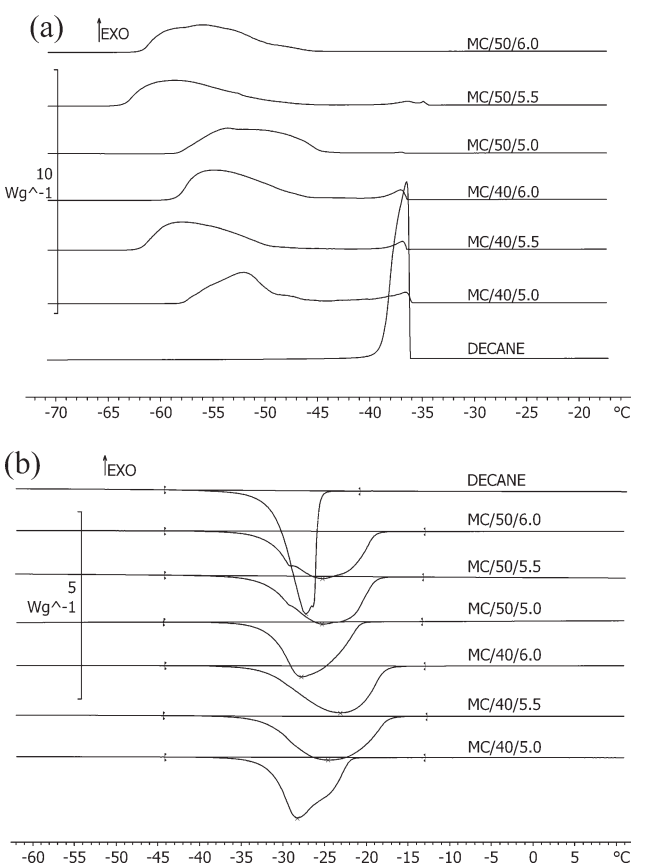

Figure 3 Thermograms for decane and the microcapsules obtained at the end of microencapsulation at 40 and 50°C and pH values of 5.0, 5.5, and 6.0: (a) decane crystallization peaks and (b) decane melting peaks. (Wg^{-1} stands for Watt per gram).

TABLE II
Accuracy and Reproducibility of the DCS Results for the Mass Percentage of the Shell Material in Microcapsule Determination for Sample MC/50/5.5

	Replicate					Average value (%)	Relative standard deviation (%)
	1	2	3	4	5		
DSC analysis: Mass percentage of shell material	5.75	5.99	6.27	6.92	6.98	6.38	8.6
Gravimetric analysis: Mass percentage of shell material	6.52	5.70	6.37	6.30	6.45	6.27	5.2

DSC analysis. Moreover, when the microencapsulation was carried out at 40°C and a pH value of 6.0, the microcapsules had not been formed yet during the first hour of microencapsulation. From the results presented in Figure 4, we perceived that for series MC/40/6.0, stable microcapsules with enough thick and hard shells were formed only after 2.5 h. The discrepancies observed up to that time (Fig. 4) were attributed to shell rupture during sampling and sample handling previous to DSC analysis. For this series, shell thickening was confirmed by the crystallization peak shapes shown in Figure 5(a), where the crystallization peak shifted toward lower temperatures with time of microencapsulation. The thicker the shells were, the larger the temperature delay for crystallization was compared to pure decane because of heat transport through shells. For series MC/50/6.0 and MC/40/5.5 (Fig. 4), the core-to-shell mass ratio after 1.5 h of microencapsulation was constant and similar to that of series MC/40/6.0 (after 2.5 h). This suggested that the shell thickness did not increase further in the period from 1.5 to 4 h. Similar crystallization peak shapes after 1.5 h of the microencapsulation process in Figure 5(b), where thermograms for series MC/50/6.0 are shown, support this suggestion. Series MC/50/5.5 samples had a slightly higher shell content in the microcapsules during the first 3 h and, thereafter, reached the same value as series MC/50/6.0 and MC/40/5.5 (Fig. 4). On the other hand, the series prepared at a pH value of 5, MC/50/5.0 and MC/40/5.0, had significantly higher shell-to-core mass ratios than the series mentioned previously through the whole timescale (Fig. 4). A decreasing trend with time, which for the series MC/50/5.0 was clearly evident, was less noticeable for series MC/40/5.0. By comparing the thermograms for series MC/50/5.0 [Fig. 5(c)] with those of series MC/40/6.0, we observed that the reason for the decreasing trend for series MC/50/5.0 should have been found elsewhere and not in the shell rupture during sampling and sample handling in the early stages of the process, as observed for series MC/40/6.0. The primary reason for the decreasing trend was the same as for the higher shell-to-core mass ratio: the lower pH value at which the microcapsules were prepared. The observed decreasing trend for series MC/50/5.0, MC/40/5.0, and MC/50/5.5 in Figure 4 were explained by the deposition of small MF particles on the surface of the microcapsules during the filtration process. Particularly in the early stages of the microencapsulation process, the surfaces of the microcapsules and small MF particles were, because of their lower level of curing, sticky. Therefore, the particles formed aggregates during filtration, and we could not separate these aggregates by washing the sample with deionized water. With increasing time of microencapsulation, the level of MF resin curing increased, particles were less sticky, and their separation by filtration and washing was possible.

However, from DCS analysis, which gave us the mass percentage of the shell material in the microcapsules with time of microencapsulation [Fig. 3(a,b) and 4], we concluded that MF shells were formed during a period of 1.5 h of the microencapsulation process, except for the series prepared at a pH value of 6.0 and a temperature 40°C, where stable microcapsules were formed only after 2.5 h. After this

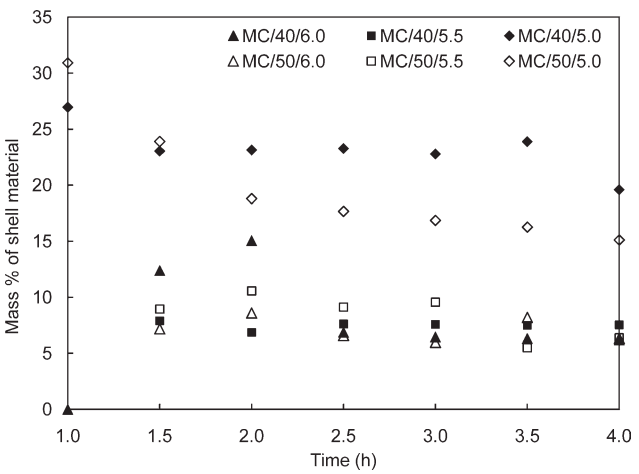

Figure 4 Mass percentage of the shell material in the microcapsules during the microencapsulation processes at 40 and 50°C and pH values 5.0, 5.5, and 6.0.

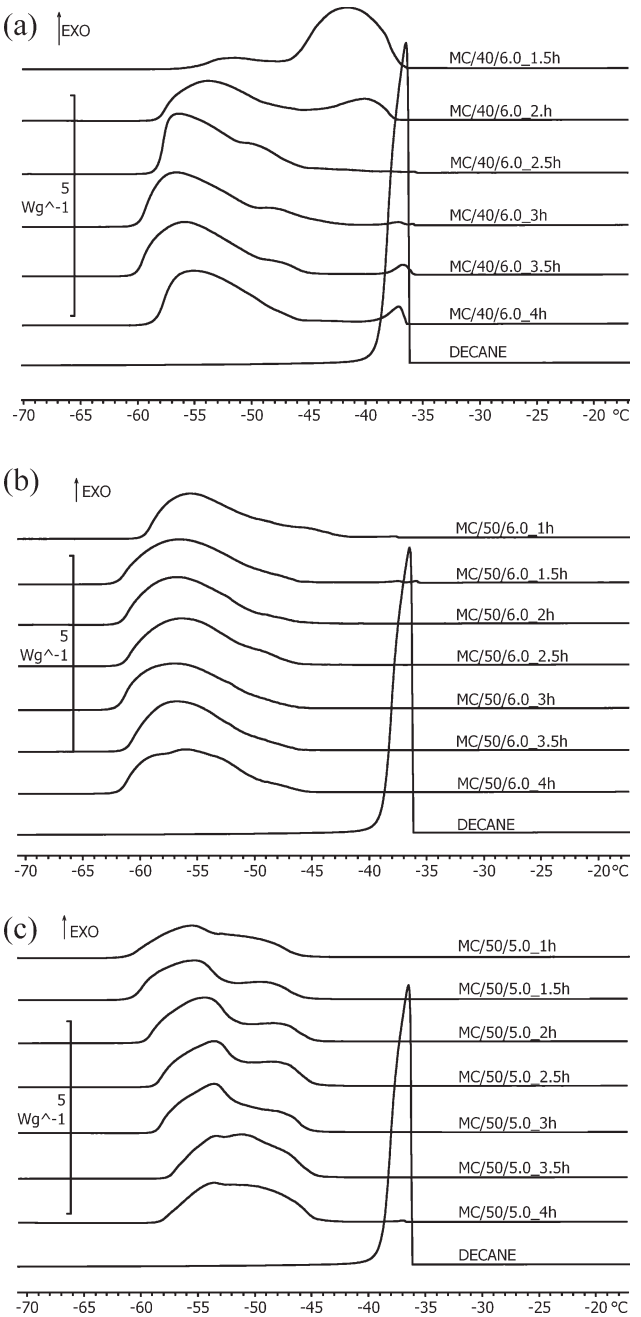

Figure 5 (a) Thermograms showing decane crystallization peaks of samples during microencapsulation process for the series (a) MC/40/6.0, (b) MC/50/6.0, and (c) MC/50/5.0. (Wg^{-1} stands for Watt per gram).

period, the microcapsule shell thickness, which was dependent on the pH value set, did not increase further.

Degree of curing of the polymer shell material

The degree of curing of MF resin forming the microcapsule shell (for the series prepared at pH 5.0) was investigated by DSC analysis. For this purpose, the area below the exothermic peaks of MF resin cross-linking or curing, which occurred between 135 and 280°C, was integrated. The microcapsule analysis required prior sample preparation because of the low mass percentage of MF resin in the microcapsules. Samples containing only MF resin from microcapsules were obtained by decane removal with the same procedure used for the gravimetric analysis described previously and, as such, used for DSC analysis. The efficiency of decane removal was verified by DSC experiments with the temperature program used for the microcapsule composition analysis. The absence of crystallization and melting peaks in the thermograms confirmed that decane was removed efficiently.

In Figure 6, thermograms for microcapsules after decane removal obtained at the end of the microencapsulation processes at 50°C and pH values of 5.0, 5.5, and 6.0 are shown, whereas the determined specific curing enthalpies are collected in Table II. The *specific curing enthalpy*, that is, the released heat in the curing process per gram of MF resin, decreased with decreasing pH value, as expected. A lower specific curing enthalpy signified a higher degree of curing of MF resin at the end of the microencapsulation process. The exothermic peaks (Fig. 6) due to MF resin curing of samples MC/50/5.0 and MC/50/5.5 occurred in the temperature interval between 135 and 280°C, whereas the peak for sample MC/50/6.0 arose between 205 and 280°C. We presumed these differences were due to different curing reactions, which occurred during the DSC experiments because we expected that samples MC/50/5.0 and MC/50/5.5 contained a higher amount of methylene bridges than sample MC/50/6.0. The thermograms of MF shells sampled during the microencapsulation process had peaks in the same temperature intervals as the thermograms of MF shells sampled at the end

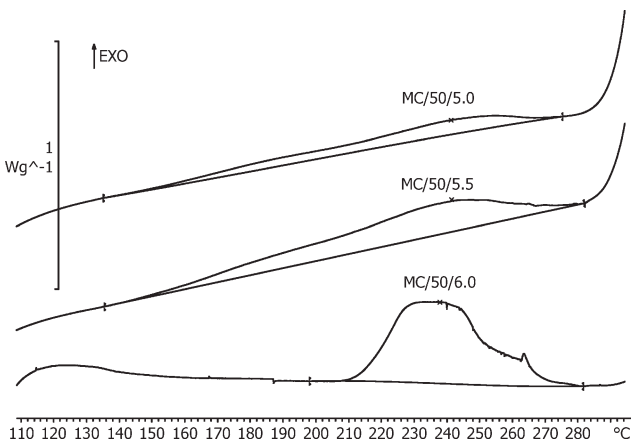

Figure 6 Thermograms showing the MF resin curing after decane removal for the microcapsules obtained at the end of the microencapsulation processes at 50°C and pH values 5.0, 5.5, and 6.0. (Wg^{-1} stands for Watt per gram).

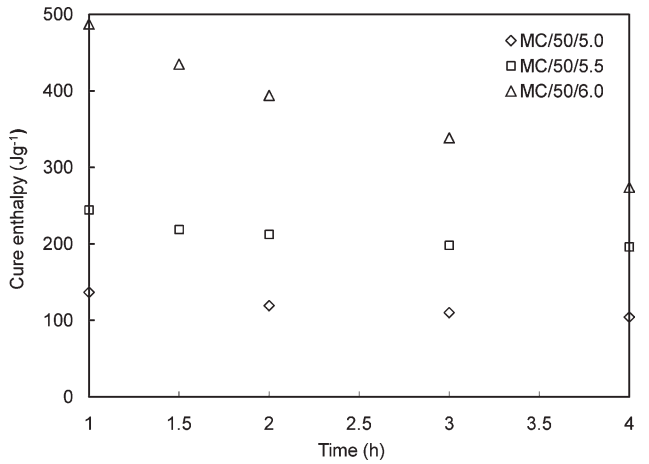

Figure 7 Curing enthalpy of the shell material of the microcapsules during microencapsulation processes at 50°C and pH values 5.0, 5.5, and 6.0.

of the process. Variations in the specific curing enthalpy of shell material in the microcapsules during microencapsulations carried out at different pH values are depicted in Figure 7. As shown, the curing enthalpy decreased and, therefore, the degree of curing increased during the microencapsulation processes. The decreasing trend was clearly evident for series MC/50/6.0, whereas for series MC/50/5.0 and MC/50/5.5, the degree of resin curing changed only a little during the last 2 h of the process. We concluded that at a pH value of 6, the polycondensation reactions and, consequently, also separation, deposition, and crosslinking of MF resin on the surface of the dispersed phase were slower. Nonetheless, this was confirmed by SEM analysis, where a thinner shell and fewer small MF particles of spherical shape for series MC/50/6.0 were observed.

CONCLUSIONS

DSC analysis in combination with SEM analysis was revealed as an effective tool for the investigation of microencapsulation processes with MF resin. For DSC investigation purposes, decane as a core material, which showed crystallization and melting peaks in the DSC thermograms, was chosen. By comparing the DSC thermograms of pure decane to those of microcapsules, we observed some evident divergences in decane crystallization and the melting peak temperature, shape, and width. The divergences were ascribed to different conditions for heat transport in the microcapsule samples and to intermolecular interactions between decane and MF resin on the core–shell interfacial area. With thicker MF shells, larger temperature delays for crystallization (compared to pure decane) were observed. Moreover, it was possible to distinguish between the signals of decane located inside and outside of the microcapsules. From the integrals of the decane melting peak for pure decane and the microcapsule samples, the mass percentage of shell material in the microcapsules was calculated. The mass percentage of shell material in the microcapsules did not increase after 1.5 h of microencapsulation. However, it was higher when the microcapsules were prepared at a lower pH value. These observations were confirmed by the results of gravimetric analysis and SEM analysis, which illustrated not only a larger shell thickness but also a major amount of small MF particles on the shell surfaces of the microcapsules prepared at lower pH values. However, the so called raspberry-like surface morphology was not observed, and we assumed that its formation was prevented by the use of a high emulsifier concentration and by the constant pH value of the continuous medium. By DSC analysis, the degree of curing of MF resin forming the microcapsule shell was also investigated. For this purpose, the area below the exothermic peaks of the MF resin crosslinking or curing, which occurred between 135 and 280°C, was integrated. A lower specific curing enthalpy signified a higher degree of curing of MF resin. As expected, we observed that the degree of curing increased during the microencapsulation process and that it was the highest when the microcapsules were fabricated at the lowest pH value.

References

1. Ghosh, S. K. In Functional Coatings; Ghosh, S. K., Ed.; Wiley-VCH: Weinheim, 2006; Chapter 1.
2. Thies, C. In Microencapsulation: Methods and Industrial Applications; Benita, S., Ed.; Marcel Dekker: New York, 1996; Chapter 1.
3. Dietrich, K.; Bonatz, E.; Geistlinger, H.; Herma, H.; Nastke, R.; Purz, H. J.; Schlawne, M.; Teige, W. Acta Polym 1989, 40, 325.
4. Lee, H. Y.; Lee, S. J.; Cheong, I. W.; Kim, J. H. J Microencapsulation 2002, 19, 559.
5. Hong, K.; Park, S. Mater Chem Phys 1999, 58, 128.
6. Hwang, J. S.; Kim, J. N.; Wee, Y. J.; Yun, J. S.; Jang, H. G.; Kim, S. H.; Ryu, H. W. Biotechnol Bioprocess Eng 2006, 11, 332.
7. Hwang, J. S.; Kim, J. N.; Wee, Y. J.; Yun, J. S.; Jang, H. G.; Kim, S. H.; Ryu, H. W. Biotechnol Bioprocess Eng 2006, 11, 391.
8. Lakkis, J. M. Encapsulation and Controlled Release Technologies in Food Systems; Wiley-Blackwell: Oxford, 2007.
9. Yuan, L.; Liang, G. Z.; Xie, J. Q.; He, S. B. Colloid Polym Sci 2007, 285, 781.
10. Yuan, Y. C.; Rong, M. Z.; Zhang, M. Q. Polymer 2008, 49, 2531.
11. Yuan, L.; Liang, G. Z.; Xie, J. Q.; Li, L.; Guo, J. J Mater Sci 2007, 42, 4390.
12. Yuan, L.; Liang, G.; Xie, J.; Li, L.; Guo, J. Polymer 2006, 47, 5338.
13. Luo, W. J.; Yang, W.; Jiang, S.; Feng, J. M.; Yang, M. B. Polym Degrad Stab 2007, 92, 1359.
14. Salaün, F.; Vroman, I. Eur Polym J 2008, 44, 849.

15. Wang, Z.; Wu, K.; Hu, Y. Polym Eng Sci 2008, 48, 2426.
16. You, M.; Zhang, X. X.; Li, W.; Wang, X. C. Thermochim Acta 2008, 472, 20.
17. Li, W.; Zhang, X. X.; Wang, X. C.; Niu, J. J. Mater Chem Phys 2007, 106, 437.
18. Su, J. F.; Huang, Z.; Ren, L. Colloid Polym Sci 2007, 285, 1581.
19. Fan, Y. F.; Zhang, X. X.; Wu, S. Z.; Wang, X. C. Thermochim Acta 2005, 429, 25.
20. Sgraja, M.; Blömer, J.; Bertlilng, J.; Jansens P. J. J Appl Polym Sci 2008, 110, 2366.
21. Su, J. F.; Wang, L. X.; Ren, L.; Huang Z. J Appl Polym Sci 2007, 103, 1295.
22. Su, J. F.; Wang, L. X.; Ren L. J Appl Polym Sci 2006, 101, 1522.
23. Kumar, A.; Katiyar, V. Macromolecules 1990, 23, 3729.
24. Choi, J. K.; Lee, J. G.; Yang, H. S. Theor Appl Chem Eng 2002, 8, 2493.
25. Zhang, X. X.; Fan, Y. F.; Tao, X. M.; Yick, K. L. Mater Chem Phys 2004, 88, 300.
26. Lee, S. H.; Yoon, S. J.; Kim, Y. G.; Choi, Y. C.; Kim, J. H.; Lee, J. G. Korean J Chem Eng 2007, 24, 332.
27. Wang, H.; Yuan, Y.; Rong, M.; Zhang, M. Colloid Polym Sci 2009, 287, 1089.
28. Salaün, F.; Devaux, E.; Bourbigot, S.; Rumeaud, P. Chem Eng J 2009, 155, 457.
29. Dietrich, K.; Bonatz, E.; Nastke, R.; Herma, H.; Walter, M.; Teige, W. Acta Polym 1990, 41, 91.
30. Zhang, H.; Wang, X. Colloids Surf A 2009, 332, 129.
31. Yu, F.; Chen, Z. H.; Zeng, X. R. Colloid Polym Sci 2009, 287, 549.
32. Yan, L.; ShuiLin, C. Color Technol 2003, 119, 37.
33. Kamio, E.; Yonemura, S.; Ono, T.; Yoshizawa, H. Langmuir 2008, 24, 13287.
34. Kamio, E.; Kato, A.; Yonemura, S.; Ono, T.; Yoshizawa, H. Colloid Polym Sci 2008, 286, 787.
35. Jang, I. B.; Sung, J. H.; Choi, H. J. J Mater Sci 2005, 40, 1031.
36. Daiguji, H.; Makuta, T.; Kinoshita, H.; Oyabu, T.; Takemura, F. J Phys Chem B 2007, 111, 8879.
37. Li, W.; Wang, J.; Wang, X.; Wu, S.; Zhang, X. Colloid Polym Sci 2007, 285, 1691.
38. Dubernet, C. Thermochim Acta 1995, 248, 259.